

# Interhemispheric differences in denitrification and related processes affecting polar ozone

M. L. Santee, w. G. Read, J. W. Waters, L. Froidevaux, G. L. Manney,  
D. A. Flower, R. F. Jarnot, R. S. Harwood\*, G. E. Peckham<sup>†</sup>

Jet Propulsion Laboratory, California Institute of Technology, Pasadena, California 91109, USA

\*Department of Meteorology, Edinburgh University, Edinburgh EH9 3JZ, UK

<sup>†</sup> Department of Physics, Heriot Watt University, Edinburgh ED14 4AS, UK

The severe depletion of stratospheric ozone over Antarctica<sup>1,2</sup> in late winter and early spring is caused<sup>3</sup> by enhanced ClO abundances<sup>4,5</sup> arising from heterogeneous reactions on polar stratospheric clouds (PSCs). ClO abundances comparable to those over Antarctica have also been observed throughout the Arctic vortex<sup>6</sup>, but the accompanying loss of Arctic ozone has been much less severe<sup>7</sup>. A major factor influencing ClO abundances is denitrification – the removal of nitrogen from the lower stratosphere through gravitational settling of PSC particles containing HNO<sub>3</sub>. Recently, measurements of gas-phase HNO<sub>3</sub> have been obtained from the Microwave Limb Sounder (MLS) onboard the Upper Atmosphere Research Satellite (UARS). MLS HNO<sub>3</sub>, H<sub>2</sub>O, ClO, and O<sub>3</sub> provide the first simultaneous common - calibrated global measurements directly showing the correlations between denitrification, dehydration and enhanced reactive chlorine affecting stratospheric ozone. The extent, degree, and duration of these processes have now been observed over an annual cycle and found to be much greater in the Antarctic than in the Arctic, consistent with previous observations<sup>16</sup> that were more limited in temporal and spatial scale. These results emphasize the importance of denitrification in polar ozone loss.

The MLS instrument<sup>17</sup> acquires stratospheric measurements which are not degraded by PSCs or aerosols<sup>18</sup>. MLS observations of  $\text{HNO}_3$ <sup>6,19</sup>,  $\text{O}_3$ <sup>6,19,20</sup>, and  $\text{H}_2\text{O}$ <sup>21</sup> have been reported previously.  $\text{HNO}_3$ , which was a secondary MLS measurement objective<sup>18</sup>, is a minor contributor in the 205 GHz spectral bands used to measure  $\text{O}_3$  and  $\text{ClO}$ . Vertical profiles of gas phase  $\text{HNO}_3$  are now being retrieved, resulting in improved fits to the radiometric data [W. G. Read *et al.*, in preparation]. The Cryogenic Limb Array Etalon Spectrometer (CLAES) onboard UARS also measures  $\text{HNO}_3$ <sup>22</sup>. Initial comparisons of MLS and CLAES  $\text{HNO}_3$  generally show good qualitative agreement, with some differences (particularly in the southern hemisphere autumn) still under investigation. The estimated precision of MLS lower stratospheric  $\text{HNO}_3$  presented here is  $\sim 2$  p.p.b.v. (parts per  $10^9$  by volume) and the absolute accuracy is  $\sim 30\%$ . The **1120** measurements are shown at lower altitudes than in ref. 21, but have sufficient precision to qualitatively follow the progression of dehydration.

Figure 1 shows the evolution of MLS  $\text{HNO}_3$ ,  $\text{ClO}$ ,  $\text{O}_3$ , and  $\text{H}_2\text{O}$  in the southern hemisphere in 1992, displayed on the 465 K isentropic surface ( $\sim 20$  km altitude) along with contours of potential vorticity characterizing the polar vortex boundary. The vortex is well established by 28 April<sup>23</sup>, with accumulation of  $\text{HNO}_3$  and  $\text{O}_3$  evident in its interior, as expected from diabatic descent<sup>24</sup>. Temperatures are still above the PSC formation threshold, and chlorine has not yet been activated.

By 2 June (the beginning of an MLS south looking period), temperatures over a broad region are low enough ( $\leq 195$  K) for the formation of Type 1 (nitric acid trihydrate, NAT) PSCs<sup>25</sup>. While ozone abundances inside the vortex have increased since late April, a deficit in gas phase  $\text{HNO}_3$  has developed coincident with the lowest temperatures. A similar decrease is not seen in  $\text{H}_2\text{O}$ . Although there has been some suggestion<sup>26</sup> that denitrification occurred prior to dehydration in the 1987 Antarctic winter, most previous Antarctic observations have shown the processes of denitrification and dehydration to be coupled<sup>8,9,15,27</sup>. Theoretical studies<sup>28,29</sup> have found that the sedimentation rate of  $\text{HNO}_3$  particles can be sufficiently rapid given low cooling rates or cooling to just below the

NAT' condensation point for substantial  $\text{HNO}_3$  loss to occur over short timescales and independent of ice particle formation. Based on data collected during the 1987 southern winter, Salawitch *et al.* calculate that extensive denitrification could have occurred by 15 June, with significant dehydration occurring later. The MLS data support the idea that denitrification can precede significant dehydration over Antarctica.

On 17 August, MLS observed<sup>19</sup> ClO values as high as 2 p.p.b.v. in most of the region poleward of 60°S, and a ring of low  $\text{O}_3$  coincident with the highest ClO abundances. The area of temperatures low enough ( $\leq 188$  K) for Type 11 (water ice) PSCs<sup>25</sup> encompasses most of the Antarctic continent. Throughout this region, gas-phase  $\text{HNO}_3$  values are extremely low ( $\leq 2$  p.p.b.v.). A 'collar' of high  $\text{HNO}_3$  ( $\geq 10$  p.p.b.v.) is seen just outside the low temperature region, consistent with previous aircraft observations<sup>8,9</sup> and co-located CLAES measurements<sup>22</sup>. The outer boundary of enhanced ClO roughly corresponds to the inner edge of the  $\text{HNO}_3$  collar region, as expected from the conversion of reactive chlorine into reservoir form ( $\text{ClONO}_2$ ) through reaction with  $\text{NO}_2$  released by  $\text{HNO}_3$  photolysis. The  $\text{H}_2\text{O}$  map indicates that intense dehydration has also now occurred within the low-temperature zone.

Lower stratospheric temperatures warmed above the threshold for Type 1 PSC formation the last week in September<sup>30</sup>. MLS measurements on 1 November (the beginning of the next south looking period) show that, although the elevated ClO abundances have receded, the ozone loss that developed in September<sup>6,19,20</sup> and the  $\text{HNO}_3$  deficit persist. The depressed  $\text{HNO}_3$  values at this time imply that irreversible removal of  $\text{HNO}_3$  (denitrification) has occurred.

This pattern of denitrification is not seen in the 1992-1993 northern polar vortex (Figure 2). In contrast to the southern hemisphere at the comparable time, on 26 October the northern vortex is not established at 465 K. By 3 December the vortex has increased substantially in size and strength [*G. L. Manney et al.*, in preparation]. Except for a small

area over southern F inland, temperatures remain too high for PSCs and ClO is not enhanced. Lower stratospheric O<sub>3</sub> and HNO<sub>3</sub> have accumulated inside the vortex, and there is no evidence that denitrification has been initiated.

The most striking differences between the hemispheres occur in late winter. While the southern vortex in August is nearly centered over the pole, the northern vortex in February is distorted, with the southernmost portion covering most of Europe on 22 February. ClO abundances are generally enhanced (> 1 p.p.b.v.) throughout the vortex, but O<sub>3</sub> values remain high, suggesting that the replenishment by diabatic descent exceeds the destruction by chlorine chemistry. Between Greenland and Scandinavia there is a low temperature area in which gas phase HNO<sub>3</sub> abundances are low (~ 5-9 p.p.b.v.) relative to the remainder of the vortex (~ 10 - 14 p.p.b.v.). This low temperature, low HNO<sub>3</sub> region persists for only a few days (not shown). There is no corresponding perturbation in O<sub>3</sub> or ClO, implying that the sequestration of gas phase HNO<sub>3</sub> in NAT PSCs, rather than intrusion of lower latitude air or uplift of the isentropes, causes the observed HNO<sub>3</sub> decrease. Compared to the Antarctic (Figure 1), the Arctic HNO<sub>3</sub> loss is less intense, more localized, and more transient, indicating that the Arctic vortex has not undergone significant denitrification. Significant dehydration is also not observed. By mid March, after two strong stratospheric warmings<sup>31</sup>, the high values of ClO have diminished. O<sub>3</sub> abundances are lower than in February, but the depletion is much less severe than in the southern vortex between August and September<sup>7</sup>. The continued presence of HNO<sub>3</sub> throughout the Arctic winter moderates the destruction of ozone by providing a source of NO<sub>2</sub> to quench ClO.

Under present climate conditions, Arctic winter temperatures remain below the Type 1 PSC threshold sufficiently long for lower stratospheric chlorine to be substantially converted to reactive form. However, they do not fall low enough, or stay low long enough, for sedimentation by either Type 1 or Type 1 PSC particles to cause extensive denitrification. Future cooling of the lower stratosphere (e.g., caused by increases in greenhouse gases)

could intensify denitrification and, while the chlorine loading remains high, lead to greater losses of Arctic ozone<sup>32,33</sup>.

1. Farman, J. C., Gardiner, B.G. & Shanklin, J.D. *Nature* **315**, 207-210 (1985).
2. Stolarski, R. S. *et al. Nature* **322**, 808-811 (1986).
3. Solomon, S. *Nature* **347**, 347-354 (1990).
4. deZafra, R.L. *et al. Nature* **328**, 408-411 (1987).
5. Anderson, J.G., Brune, W.J. & Proffitt, M.J. *J. geophys. Res.* **94**, 11,465-11,479 (1989).
6. Waters, J.W. *et al. Nature* **362**, 597-602 (1993).
7. Manney, G.L. *et al. Nature* (submitted).
8. Fahey, D.W., *et al. J. geophys. Res.* **94**, 16,665-16,681 (1989).
9. Toon, G.C. *et al. J. geophys. Res.* **94**, 16,571-16,596 (1989).
10. Coffey, M.T., Mankin, W.G. & Goldman, A. *J. geophys. Res.* **94**, 16,597-16,613 (1989).
11. Arnold, F. *et al. Nature* **342**, 493-497 (1989).
12. Toon, G.C. *et al. J. Geophys. Res. Lett.* **17**, 437-440 (1990).
13. Mankin, W. G. *et al. Geophys. Res. Lett.* **17**, 473-476 (1990).
14. Kawa, S.R. *et al. Geophys. Res. Lett.* **17**, 485-488 (1990).
15. Kelly, K.K. *et al. J. geophys. Res.* **94**, 11,357-11,371 (1989).
16. Kelly, K. K. *et al. Geophys. Res. Lett.* **17**, 465-468 (1990).
17. Barath, F.T. *et al. J. geophys. Res.* **98**, 10,751-10,762 (1993).
18. Waters, J.W. in *Atmospheric Remote Sensing by Microwave Radiometry* (ed Janssen, M.A.) ch.8 (Wiley, New York, 1993).
19. Waters, J.W. *et al. Geophys. Res. Lett.* **20**, 1219-1222 (1993).
20. Manney, G.L. *et al. Geophys. Res. Lett.* **20**, 1279-1282 (1993).
21. Harwood, R.S. *et al. Geophys. Res. Lett.* **20**, 1231-1234 (1993).
22. Roche, A.E., Kumer, J.L., Mergenthaler, J.L. *Geophys. Res. Lett.* **20**, 1223-1226 (1993).
23. Manney, G. L. & Zurek, R.W. *Geophys. Res. Lett.* **20**, 1275-1278 (1993).

24. Schoeberl, M.J. & Hartmann, D.L. *Science* **251**, 461-462 (1991).
25. Turco, R.P., Toon, O.B. & Hamill, P. *J. geophys. Res.* **94**, 16,493-16,510 (1989).
26. Hamill, P. & O.B. Toon *Geophys. Res. Lett.* **17**, **441444** (1990).
27. Fancly, D.W. *et al. Nature* **344**, 321-324 (1990).
28. Salawitch, R.L., Gobbi, G.P., Wofsy, S.C. & McElroy, M.B. *Nature* **339**, 525-527 (1989).
29. Toon, O.B., Turco, R.P. & Hamill, P. *Geophys. Res. Lett.* **17**, 445-448 (1990).
30. National Oceanic and Atmospheric Administration, Climate Analysis Center, National Meteorological Center, *Southern Hemisphere Winter Summary, 1992, Selected Indicators of Stratospheric Climate* (Washington, DC, 1992).
31. Manney, G.L. *et al. Geophys. Res. Lett.* (in the press).
32. Brune, W.H. *et al. Science* **252**, 1260-1266 (1991).
33. Austin, J., Butchart, N. & Shine, K.P. *Nature* **360**, 221-225 (1992).

ACKNOWLEDGEMENTS. We thank M. R. Schoeberl for encouraging us to pursue the MLS HNO<sub>3</sub> measurement; A. E. Roche and the CLAES team for discussions and comparisons of HNO<sub>3</sub>; NMC Climate Analysis Center personnel, especially M. E. Gelman and A. J. Miller, for making NMC data available to the UARS project; our MLSC colleagues, especially T. Lungu and K. P. Thurstans. M. L. Santee gratefully acknowledges a Resident Research Associateship from the National Research Council. The work at JPL Caltech was sponsored by NASA, and the work at EU and HWU by SERC.

## Figure Captions

FIG. 1. Maps of MLS  $\text{NO}_3$ ,  $\text{ClO}$ ,  $\text{O}_3$ , and  $\text{H}_2\text{O}$  for selected days during the 1992 southern winter, interpolated onto the 465 K potential temperature ( $\theta$ ) surface using United States National Meteorological Center (NMC) temperatures. These days were chosen to illustrate conditions prior to, during, and after the period in which lower stratospheric temperatures were low enough for PSCs. The maps are polar orthographic projections extending to the equator, with the Greenwich meridian at the top and dashed black circles at  $30^\circ\text{S}$  and  $60^\circ\text{S}$ . No measurements were obtained in the white area poleward of  $80^\circ\text{S}$ . The thick black contour concentric with this region on the  $\text{ClO}$  maps identifies the edge of daylight for the measurements. Only data from the “day” side of the orbit are shown for  $\text{ClO}$ ; maps for all other species include data from a 24 hour period. Thin black lines show NMC temperature contours of 195 K (outer contour) and 188 K (inner contour), the approximate threshold temperatures<sup>25</sup> for Type I and Type II PSCs, respectively. Also superimposed (in white) on each of the maps are two contours of potential vorticity (PV), calculated from NMC temperature and geopotential height fields. The outer contour ( $-2.5 \times 10^{-5} \text{ Km}^2\text{kg}^{-1}\text{s}^{-1}$ ) represents the approximate edge of the polar vortex during winter when it is well-established<sup>20</sup>; inclusion of the inner contour ( $-3.0 \times 10^{-5} \text{ Km}^2\text{kg}^{-1}\text{s}^{-1}$ ) provides information on the steepness of the PV gradient, indicating the strength of the vortex.

FIG. 2. As in Fig. 1, but for selected days during the 1992-1993 northern winter, with the Greenwich meridian at the bottom, and positive PV contour values.



# 1992 Southern Winter - MLS data at 465 K

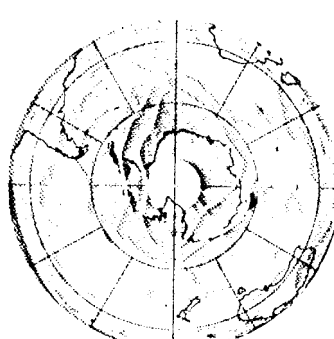
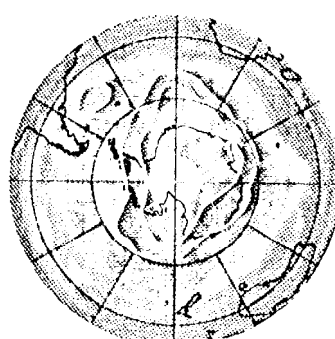
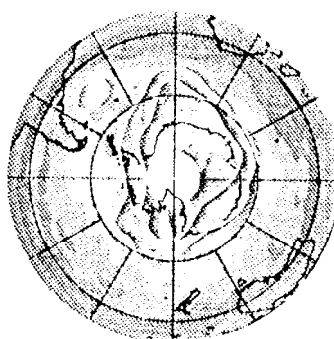
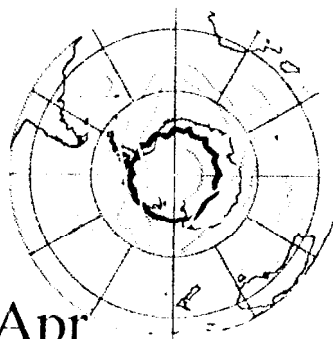
ClO

O3

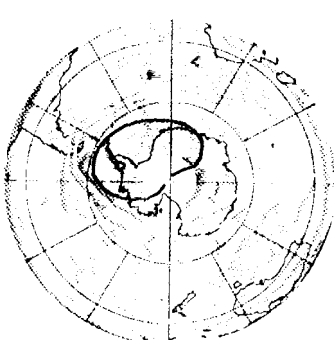
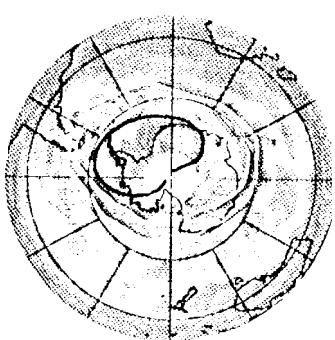
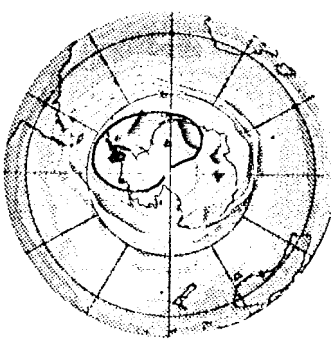
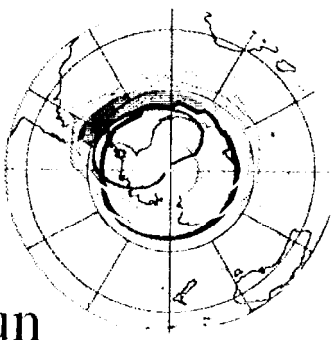
HNO3

H2O

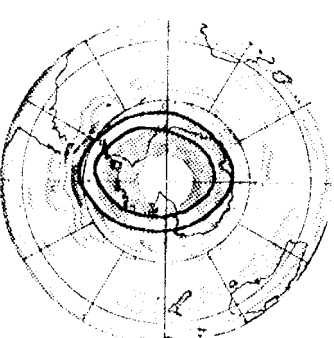
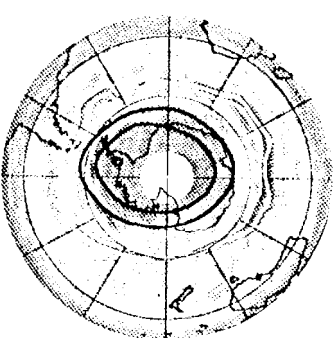
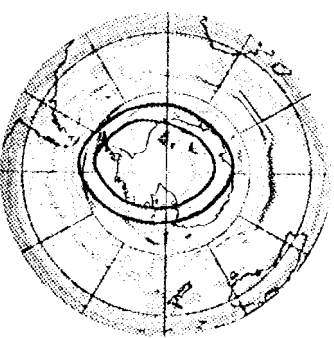
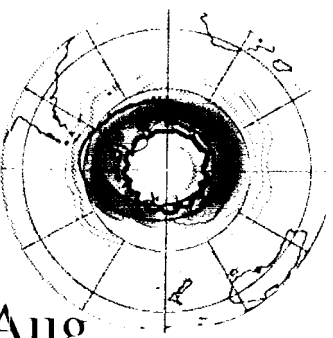
28 Apr



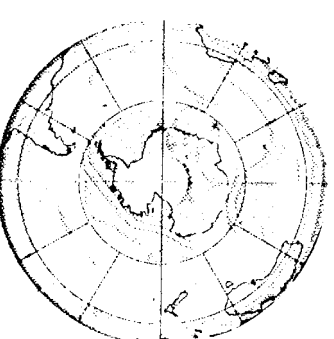
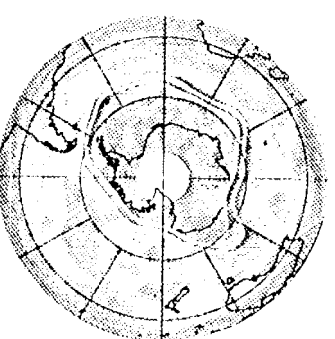
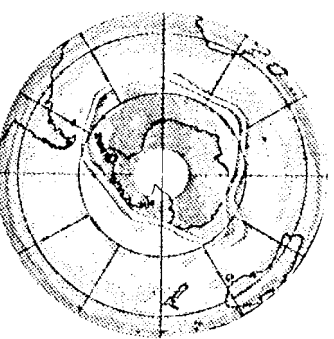
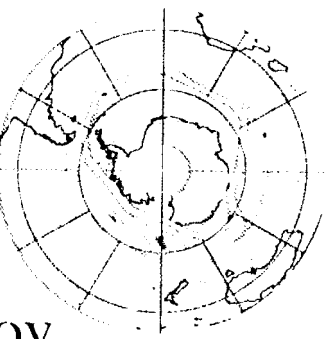
2 Jun



17 Aug



1 Nov



0.25 p.p.b.v. 2.25

1.0 p.p.m.v. 3.4

0.5 p.p.b.v. 13.5

2.5 p.p.m.v. 6.5

# 1992-1993 Northern Winter - MLS data at 465 K

ClO

O3

HNO3

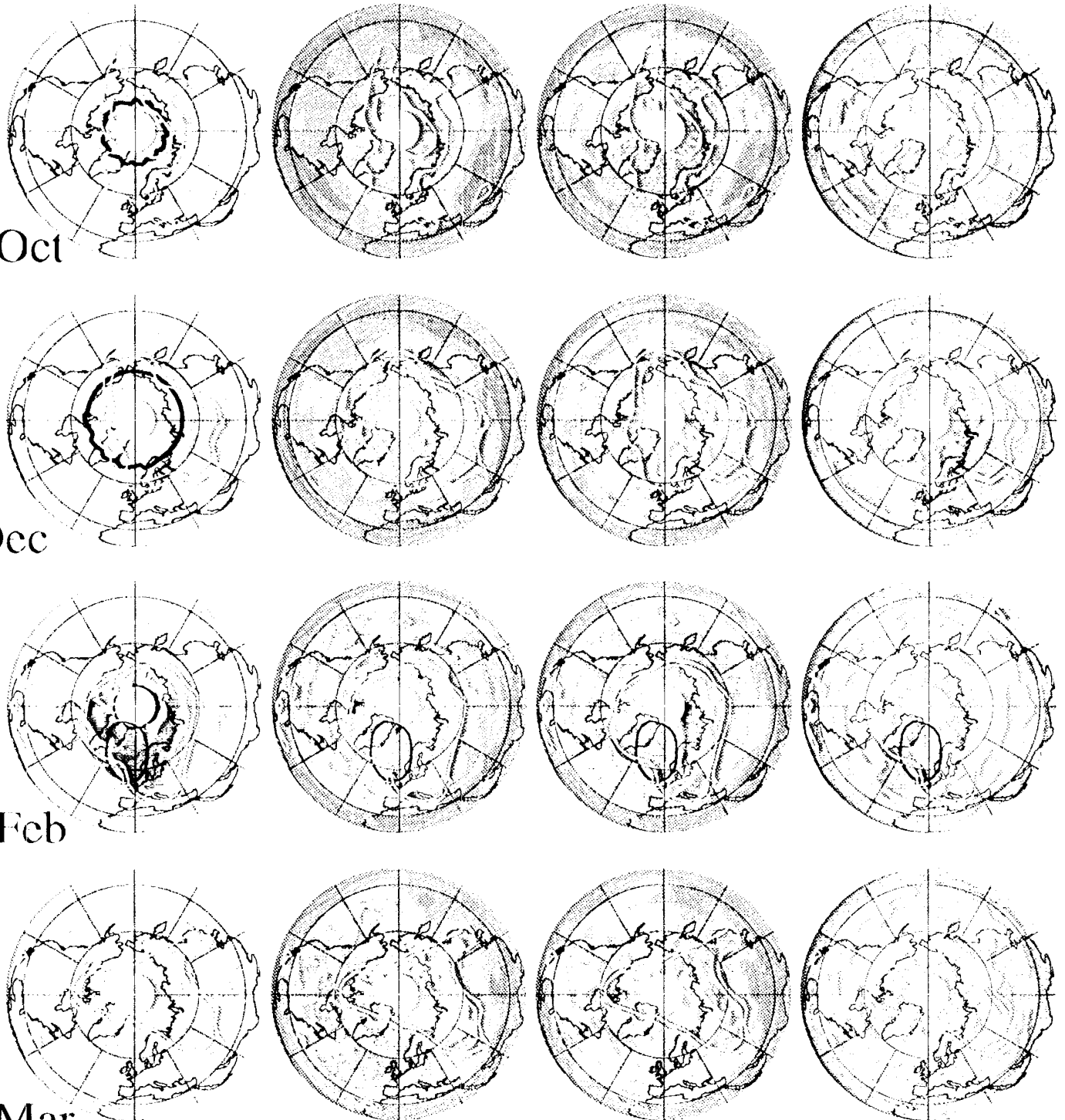
H2O

26 Oct

3 Dec

22 Feb

14 Mar



0.25 p.p.b.v. 2.25

1.0 p.p.m.v. 3.4

0.5 p.p.b.v. 13.5

2.5 p.p.m.v. 6.5